

A Compact Acousto-Optical Module for Hyperspectral Imaging Systems

Milana Sharikova

Scientific and Technological Center of
Unique Instrumentation Russian
Academy of Sciences
Moscow, Russia
milana.fartuna@yandex.ru

Vladislav Batshev

Scientific and Technological Center of
Unique Instrumentation Russian
Academy of Sciences
Moscow, Russia
batshev_vlad@mail.ru

Alexey Kozlov

Scientific and Technological Center of
Unique Instrumentation Russian
Academy of Sciences
Moscow, Russia
akaban@mail.ru

Sergey Boritko

Scientific and Technological Center of
Unique Instrumentation Russian
Academy of Sciences
Moscow, Russia
boritko@mail.ru

Vitold Pozhar

Scientific and Technological Center of
Unique Instrumentation Russian
Academy of Sciences
Moscow, Russia
vitold@ntcup.ru

Anton Karandin

Scientific and Technological Center of
Unique Instrumentation Russian
Academy of Sciences
Moscow, Russia
karandin.av@ntcup.ru

Abstract—We present an acousto-optical module, which is characterized by small monolithic design, rather good image quality and variability of instrument function. The module is compact and USB-controlled that makes easy its integration into existing imaging systems. We demonstrate the efficiency of the module for hyperspectral imaging in the ranges 450-900 nm and 900-1700 nm. The module may be the basis of hyperspectral imagers for various applications.

Keywords—acousto-optical tunable filter; hyperspectral imaging.

I. INTRODUCTION

The most promising method for spectral imaging is based on acousto-optical tunable filters (AOTF). They have a number of important technical advantages: fast (~ 1 ms) random spectral access, high spectral resolution (the bandwidth up to 0.1 nm), the ability to modulate the signal and synthesize the transfer functions, lack of moving elements, small mass and dimensions [1-3]. They can be the basis for implementation of fundamentally new methods for visualizing objects [4].

Now, acousto-optical (AO) functional elements as well as some devices based on them, for example imaging spectrometers, are commercially available [5,6]. Typically, AOTF comprises an AO cell, input and output crossed polarizers and radiofrequency electronics for ultrasound wave generation. Its principle of operation is based on anisotropic Bragg light diffraction by a dynamic acoustic grating [7]. AOTF is capable to select the light waves in any narrow spectral range with the required transmission factor by tuning the frequency and the power of the ultrasound.

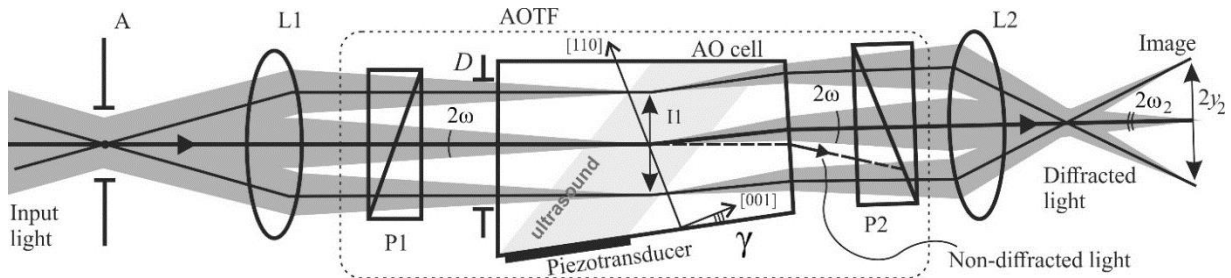


Fig. 1. Confocal scheme of the AOTF-based spectral imaging system.

The main types of aberrations caused by the AO filter are distortion, longitudinal position chromatism, and transverse chromatic shift of the image [8, 9]. In the confocal AO

II. AOTF DESIGN

One of the factors limiting the application area of AOTFs is the spectral range of tuning, limited by technological factors, usually one octave, for example, 450-900 nm, 900-1800 nm, etc. To create instruments operating in a wider spectral range, several AOTFs can be used. In this paper we show the ability to create AOTFs operating in visible and near infrared (NIR) ranges (0.45 - 0.9 μm , 0.9 - 1.7 μm) with using of the same AO cell geometry.

The shape of AO cell defines the image distortions. Moreover, these distortions also depend on the optical design of the spectral imaging device. The main types of optical aberrations caused by the AO interaction are: distortion, longitudinal chromatic image shift, transverse chromatic image drift. Aperture aberrations are also presented but negligible. In the focusing scheme without the intermediate image located inside of the AOTF the worst aberration is astigmatism [8].

In the paper [8] we show that confocal telecentric scheme provides the best image quality because of the absence of the distortion and small values of the other aberration. So, for this scheme the proposed AOTF was designed. It is shown on the Fig. 1. Lens L1 forms the intermediate image I1 of the observing object inside the AO cell. Lens L2 projects it onto the detector. To obtain the telecentric ray propagation the aperture stop should be placed to the front focal plane of the first lens L1.

Longitudinal chromatic image shift in the presented scheme could be minimized by special design of the lenses L1 and L2.

filtering scheme distortion is absent [8-10]. The position chromatism, which manifests itself in the form of defocusing images recorded at different wavelengths, depends only on

the length of the crystal and can be compensated by other optical elements.

Transverse chromatic image drift appearing in this scheme couldn't be compensated by axisymmetric elements, therefore, it should be minimized due to the inclination of the output AO cell facet. The calculations performed using the special ray-tracing module [11] show the possibility of such compensation in the AO cell made of paratellurite (TeO_2) with a cut angle $\gamma = 7^\circ$ for a wide spectral range. The residual chromatic image drift in the range of $0.45 - 1.7 \mu\text{m}$ not exceed of 1% of the image size. So, this AO cell geometry could be used in AOTF of any working spectral range within $0.45 - 1.7 \mu\text{m}$.

Spatial resolution of the AOTF is limited by the light diffraction on the input optical window and specific aberrations. The last ones are rather small. That is why we can expect image quality to be close to the diffraction limit. The maximal number of resolvable image elements in the image could be calculated as

$$N = \frac{2y_2}{\rho_{Airy}}, \quad (1)$$

where ρ_{Airy} is the radius of Airy disc, and $2y_2$ is the image size.

Considering that the intermediate image size is equal to the input window diameter D we can write

$$\frac{2y_2}{D} = \frac{\tan \omega}{\tan \omega_2}. \quad (2)$$

Airy disc radius can be found from

$$\rho_{Airy} = \frac{0.61\lambda}{\sin \omega_2}, \quad (3)$$

where λ is optical wavelength.

So, according to previous formulas and due to small angles ω and ω_2 we can write

$$N = \frac{D \tan \omega}{0.61\lambda}. \quad (4)$$

The diameter of the input window of the designed AOTF is $D = 10 \text{ mm}$. Glan-Taylor prisms are used as polarizers. They define the angular aperture of the entire AOTF which is $2\omega = 3^\circ$. Thus, the maximal number of the resolvable elements $N = 750 \times 750$ (at $\lambda = 555 \text{ nm}$) and $N = 300 \times 300$ (at $\lambda = 1.4 \mu\text{m}$).

To confirm it two AOTFs were manufactured (Fig. 2). They are completely identical except the spectral range. Their technical parameters are presented in the Table 1.

One of the modern trends in optical instrumentation is the modular concept of the devices [12]. That is why we designed AOTF as a module which, unlike commercially available AOTFs, contains all the necessary optical and electronic components (AO cell, two polarizers, generator, amplifier, piezotransducer). Our module can be inserted into the device or removed from it without any affect on it.

III. EXPERIMENTAL RESULTS

Two main parameters were checked: spectral and spatial resolution.

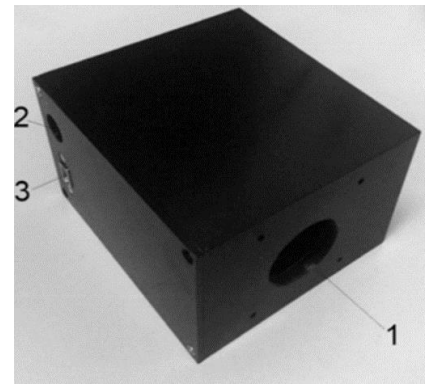


Fig. 2. The housing of the acousto-optic module: 1 - optical window, 2 - power supply socket, 3 - USB port for data exchange.

TABLE I. TECHNICAL PARAMETERS OF THE MANUFACTURED AOTFS

Parameter	AOTF #1	AOTF #2
Spectral Range	0.45 – 0.9 μm	0.9 - 1.7 μm
Spectral resolution	4 nm (at 555 nm)	50 nm (at 1.4 μm)
Spatial resolution	750×750 (at 555 nm)	300×300 (at 1.4 μm)
Light diameter	10 mm	
Angular aperture	4°	
Dimensions	75 × 82 × 52 mm ³	
Weight	0.5 kg	
Interface	UBS 2.0	
Supply voltage	12V (DC)	

To illustrate the spectral resolution of the manufactured AOTFs the transmission functions measured by a high-resolution diffraction spectrometer at various wavelengths are shown on the Fig.3.

For experimental research of fundamentally achievable quality of images formed by the AOTF-based spectral imaging system, two layouts were created: for the visible and NIR ranges. Their optical schemes are in accordance with the Fig. 1. We used standard machine-vision lenses. The input lens was focused in such a way as to obtain an image of an object located at a finite distance from the lens. As an object we used standard resolution test chart.

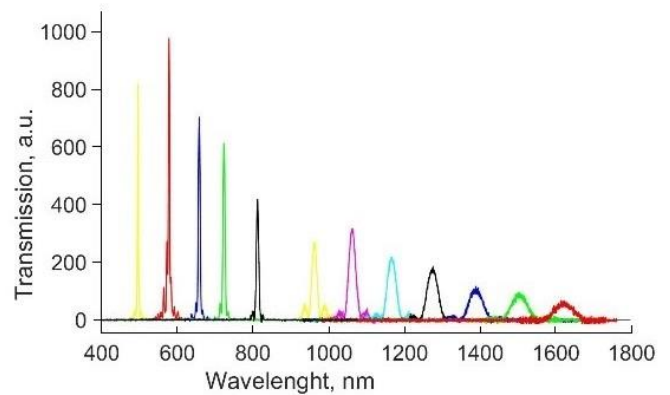


Fig. 3. Transmission windows (instrument functions) of the AOTF module.

The detector in the visible range was monochrome industrial CMOS camera TheImagingSource DMK 23UP1300 with the resolution of 1280×1024 pixels and

sensor size of $6.1 \times 4.9 \text{ mm}^2$ ($1/2''$). So, according to Table 1 the diffraction limited image resolution at $\lambda = 555 \text{ nm}$ should be $750/4.9 \text{ mm} \approx 150 \text{ mm}^{-1}$.

In the NIR range we used Allied Vision Goldeye CL-008 TEC1 camera with InGaAs 320×256 sensor and a $30 \mu\text{m}$ pixel. The sensor size is $9.6 \times 7.7 \text{ mm}^2$. The calculated

diffraction limited resolution at $\lambda = 1400 \text{ nm}$ is $300/7.7 \text{ mm} \approx 40 \text{ mm}^{-1}$.

Since the fields of view and magnifications are differ in the layouts working in the different spectral ranges, we present fragments of the obtained images in the Fig. 4. They are cropped so that the fields of view are aligned.

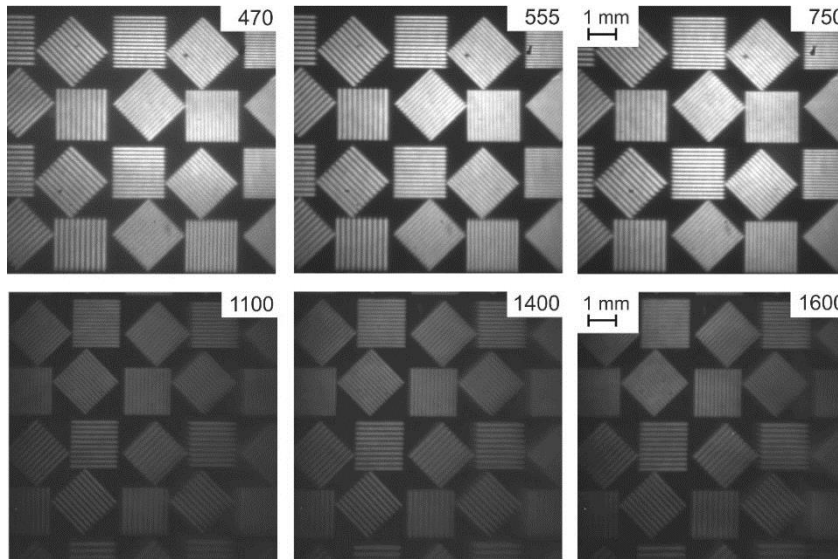


Fig. 4. Fragments of spectral images of an optical test-chart recorded at different wavelength with the AOTF modules in the confocal scheme.

Obtained series of spectral images of the test chart demonstrates a good spectral stability, high resolution and negligible distortions in the entire spectral range $0.45\text{-}1.7 \mu\text{m}$. There is a slight transverse shift of the image during tuning along the wavelength. These small offsets are not significant and can be easily corrected by spectral and spatial calibration.

The measured spatial resolution at a wavelength of 555 nm is about 80 mm^{-1} , and at a wavelength of 1400 nm - about 20 mm^{-1} . So, we can see the good compliance with calculated values.

The differences between the experimental and calculated data are primarily due to the fact that standard lenses were not used for prototyping to compensate for the distortion of the AO filter. However, even with this, it was possible to obtain the image with a high spectral and spatial resolution in both visible and NIR ranges.

IV. CONCLUSION

The main goal of this work was to develop an AOTF of modular construction provided high image quality in the visible and NIR ranges ($0.45 - 0.9 \mu\text{m}$, $0.9 - 1.7 \mu\text{m}$). It is shown that such an AOTF can be created according to the same scheme for both spectral ranges, with the same AO cell shape, using the same diffraction geometry. In particular, this makes it possible to create dual-band AOTFs [13] provided high image quality and high AO diffraction efficiency in both spectral ranges.

A correct choice of the geometry of the AO interaction and the cut angle of the crystal face provide compensation for the chromatic shift of the image and eliminates the need for refocusing during spectrum tuning.

The developed program-controlled imaging AOTFs for the most requested spectral ranges have a potential to be the basis for hyperspectral systems and imaging

spectrometers for various applications. Compact modular design makes it easy to integrate it into various optical schemes [10]. The spectral tuning module with proper spatial spectral calibration can be used for precision spatial-spectral measurements.

ACKNOWLEDGMENT

This work was performed using the equipment of the Center for Collective Use of the Scientific and Technological Center of Unique Instrumentation of the Russian Academy of Sciences [14]. The Russian Foundation for Basic Research (project 18-29-20095).

REFERENCES

- [1] N. Gupta, "Hyperspectral imager development at Army Research Laboratory," Proc. SPIE, vol. 6940, pp. 1-10, 2008.
- [2] C.N. Pannel, E.S. Wachman, D.L. Farkas, J. Ward and W. Seale, "Acousto-optic tunable filters, advances and applications to microscopy," Proc. SPIE, vol. 6088, pp. 165-173, 2005.
- [3] A.S. Machikhin, V.E. Pozhar and V.I. Batshev, "Compact AOTF-based spectral imaging system for medical endoscopic analysis," Photonics and Lasers in Medicine, vol. 2, no. 2, pp. 153-159, 2013.
- [4] L.J. Denes, M.S. Gottlieb and B. Kaminsky, "Acousto-optic tunable filters in imaging applications," Opt. Eng., vol. 37, no. 4, pp. 1262-1268, 1998.
- [5] A. Machikhin, V. Batshev, V. Pozhar and M. Mazur, "Acousto-optical full-field stereoscopic spectrometer for 3D reconstruction in arbitrary spectral intervals," Computer Optics, 2016, vol. 40, no. 6, pp. 871-877. DOI: 10.18287/2412-6179-2016-40-6-871-877.
- [6] V.P. Sherendak, I.A. Bratchenko, O.O. Myakinin, P.N. Volkhin, Y.A. Khristoforova, A.A. Moryatov, A.S. Machikhin, V.E. Pozhar, S.G. Kozlov and V.P. Zakharov, "Hyperspectral in vivo analysis of normal skin chromophores and visualization of oncological pathologies," Computer Optics, 2019, vol. 43, no. 4, pp. 661-670. DOI: 10.18287/2412-6179-2019-43-4-661-670.
- [7] A.P. Goutzoulis, D.R. Pape and S.V. Kulakov, "Design and fabrication of acousto-optic devices," New York: M. Dekker, 1994, 497 p.

- [8] A.S. Machikhin, V.I. Batshev and V.E. Pozhar, "Aberration analysis of AOTF-based spectral imaging systems," *J. Opt. Soc. Am. A*, vol. 34, no. 7, pp. 1109-1113, 2017.
- [9] S.Y. Ryu, J.-W. You, Y. Kwak and S. Kim, "Design of a prism to compensate the angular-shift error of the acousto-optic tunable filter," *Optics Express*, vol. 16, pp. 17138-17147, 2008.
- [10] D.R. Suhre, L.J. Denes and N. Gupta, "Telecentric confocal optics for aberration correction of acousto-optic tunable filters," *Applied Optics*, vol. 43, pp. 1255-1260, 2004.
- [11] V.I. Batshev, A.S. Machikhin and V.E. Pozhar, "Determining the Aberration Characteristics of Optical Systems Containing Acousto-Optical Diffraction Elements," *Technical Physics Letters*, vol. 43, no. 2, pp. 216-219, 2017.
- [12] V.E. Pozhar, M.F. Bulatov, A.S. Machikhin and V.A. Shakhnov, "Technical implementation of acousto-optical instruments: basic types," *Journal of Physics: Conference Series*, vol. 1421, no. 12058, pp. 1-8, 2019.
- [13] N. Gupta and V. Voloshinov, "Development and characterization of two-transducer imaging acousto-optic tunable filters with extended tuning range," *Applied Optics*, vol. 46, no. 7, pp. 1081-1088, 2007.
- [14] Center for Collective Use of the Scientific and Technological Center of Unique Instrumentation of the Russian Academy of Sciences [Online]. URL: <http://ckp.ntcup.ru>.